Electronic Supplementary Material (ESI) for Journal of Materials Chemistry A.

Supporting Information

Highly Selective Electrochemical CO_2 Reduction to CO Using a Redox-Active Couple on Low-Crystallinity Mesoporous $ZnGa_2O_4$ Catalyst

Meiming Zhao [a], Yaliu Gu[a], Ping Chen[a], Zhenyu Xin[a], Heng Zhu[a], Bing Wang*[a], Kai Zhu*[b], Shicheng Yan*[a] and Zhigang Zou[ac]

[a] Jiangsu Key Laboratory of Artificial Functional Materials,Eco-materials and Renewable Energy Research Center (ERERC), National Laboratory of Solid State Microstructures, Collaborative Innovation Center of Advanced Microstructures, College of Engineering and Applied Sciences, Nanjing University, No. 22 Hankou Road, Nanjing, Jiangsu 210093, P. R. China. Email: yscfei@nju.edu.cn, bingwang@nju.edu.cn

[b] School of Information Science and Engineering, Nanjing University Jinling College, No. 8, Xuefu Road, Nanjing, Jiangsu 210089, People's Republic of China. Email: zhukai@jlxy.nju.edu.cn

[c] Jiangsu Key Laboratory for Nano Technology, National Laboratory of Solid State Microstructures, School of Physics, Nanjing University, No. 22, Hankou Road, Nanjing, Jiangsu 210093, People's Republic of China

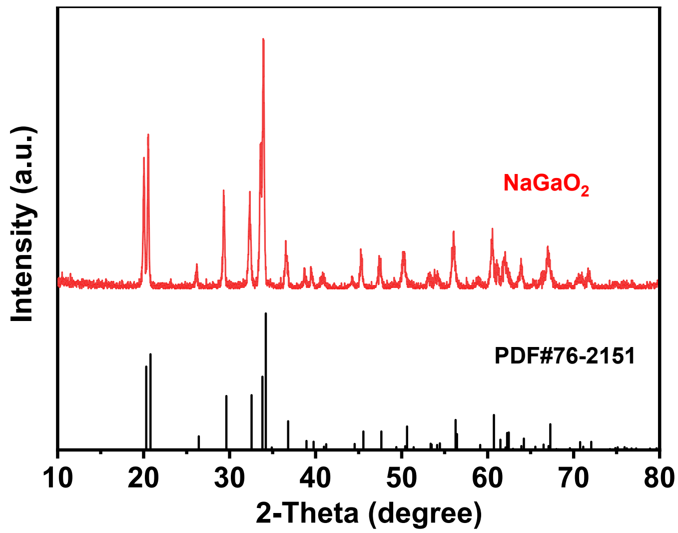

Figure S1. XRD pattern of $NaGaO_2$.

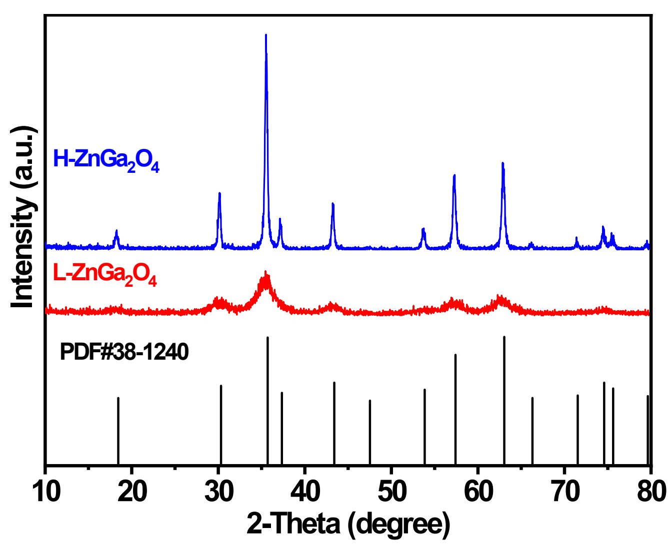

Figure S2. XRD patterns of H-$ZnGa_2O_4$ and L-$ZnGa_2O_4$.

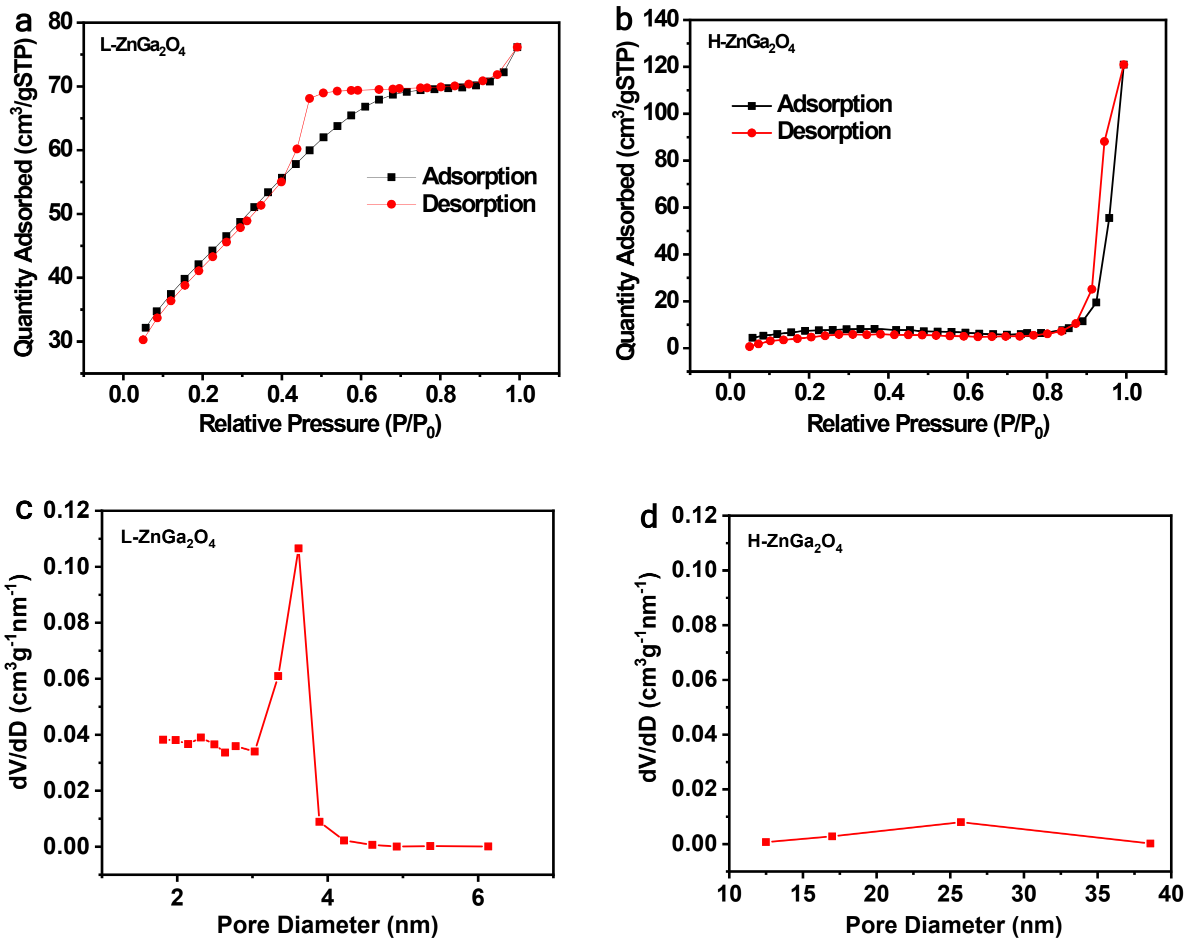

Figure S3. Nitrogen adsorption-desorption isotherms of a) L-$ZnGa_2O_4$ and b) H-$ZnGa_2O_4$. Pore diameter of c) L-$ZnGa_2O_4$ and d) H-$ZnGa_2O_4$.

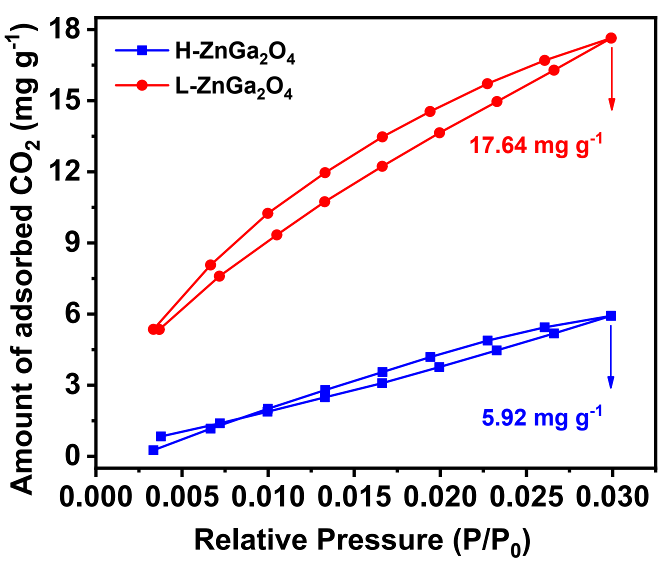

Figure S4. CO_2 adsorption capacity for the L-$ZnGa_2O_4$, H-$ZnGa_2O_4$.

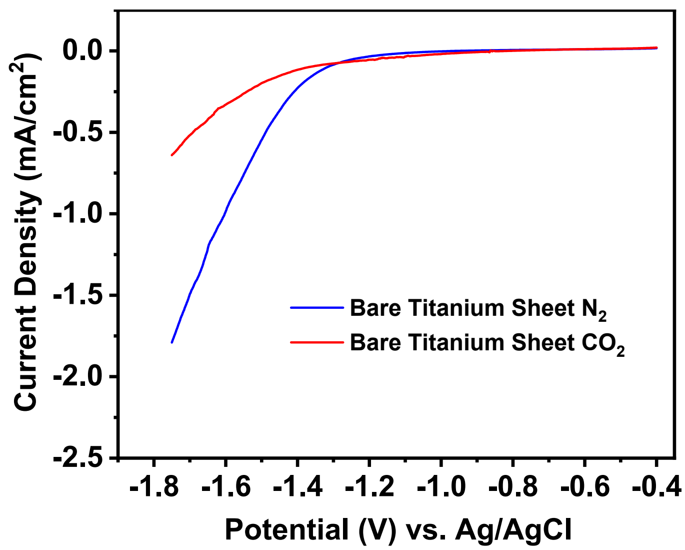

Figure S5. Polarization curves on bare titanium sheet in N_2- (blue line) or CO_2-saturated (red line) 0.1 M $KHCO_3$ solution.

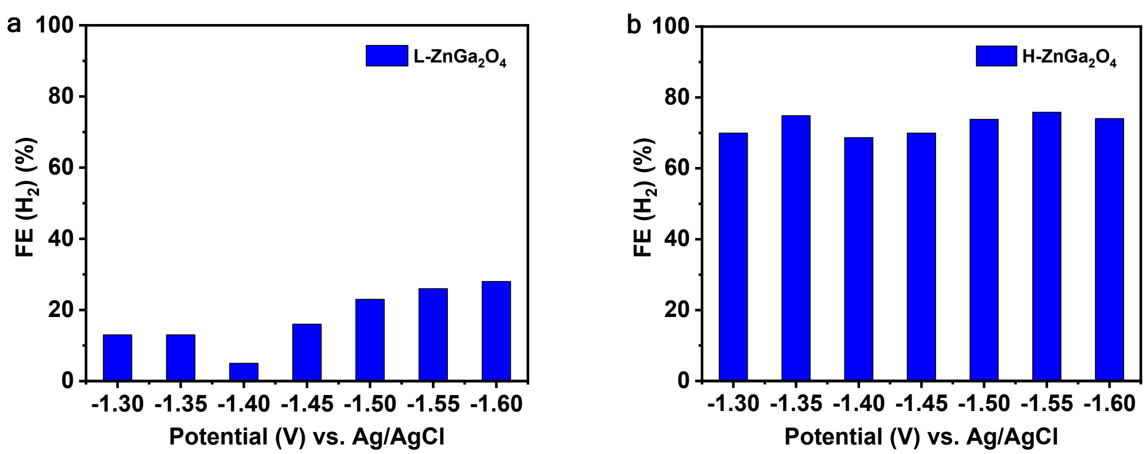

Figure S6. H_2 faradaic efficiency of a) L-$ZnGa_2O_4$ and b) H-$ZnGa_2O_4$.

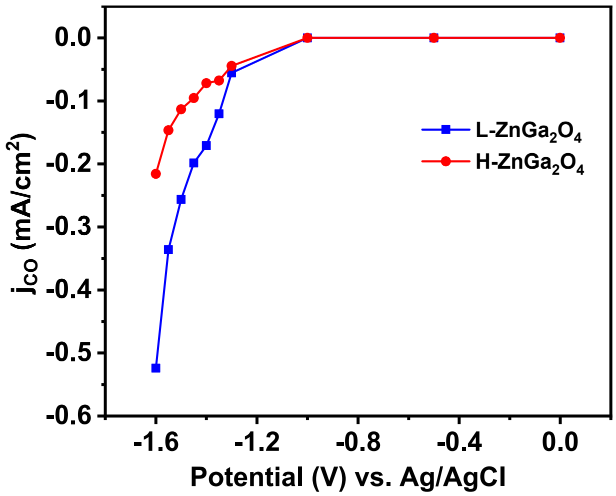

Figure S7. Partial current density of CO for L-$ZnGa_2O_4$ and H-$ZnGa_2O_4$.

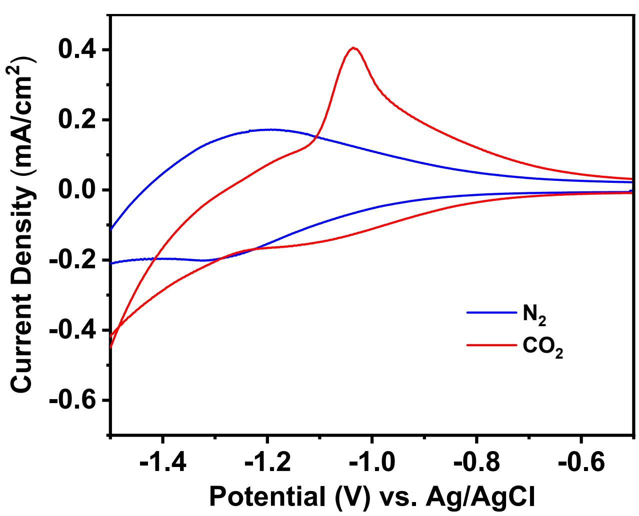

Figure S8. Redox waves of L-$ZnGa_2O_4$ in N_2 and CO_2-saturated 0.1 M $KHCO_3$ solution.

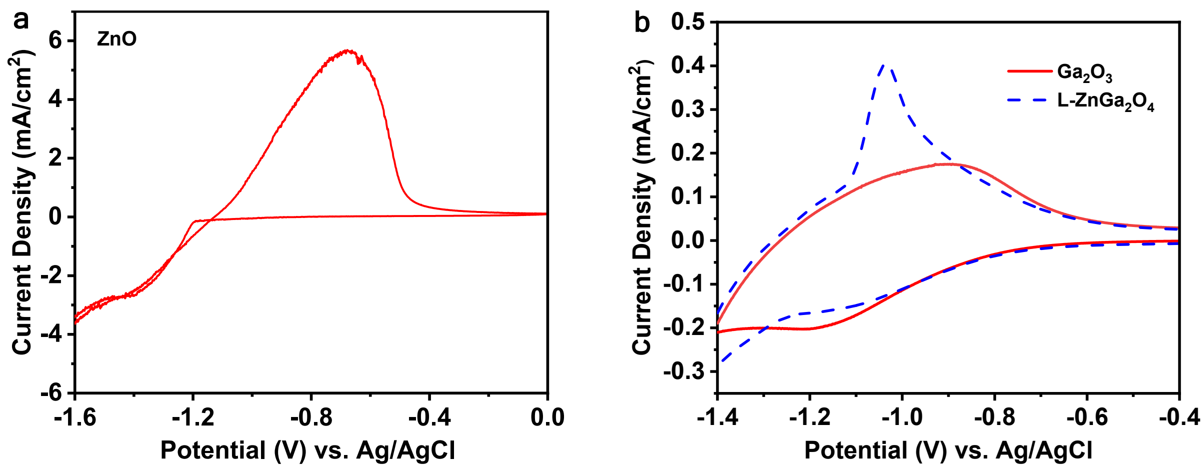

Figure S9. Oxidation peak of a) commercial ZnO, b) L-$ZnGa_2O_4$ and commercial Ga_2O_3 in CO_2-saturated 0.1 M $KHCO_3$ solution.

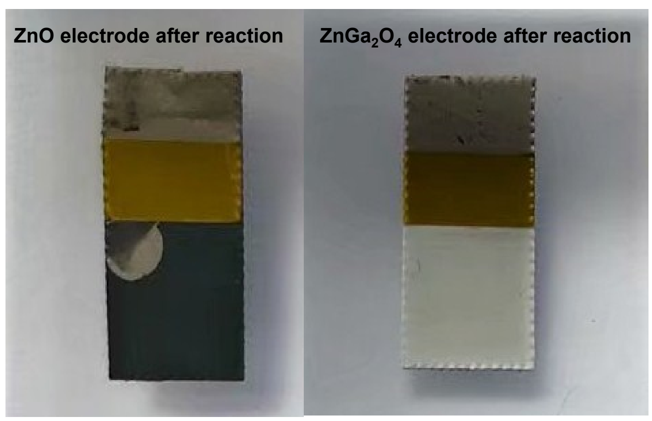

Figure S10. Photograph of ZnO electrode and $ZnGa_2O_4$ electrode after cyclic voltammogram scanning.

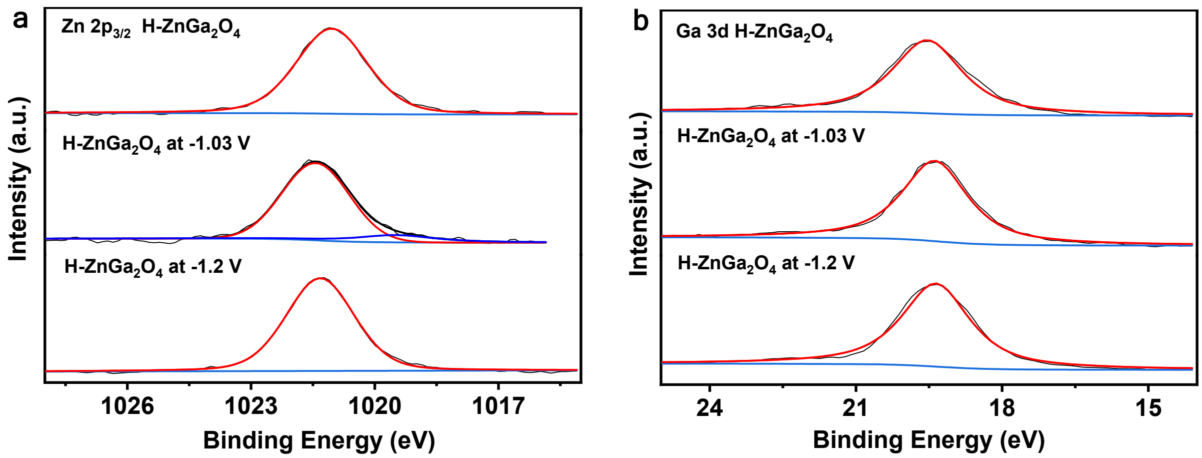

Figure S11. XPS spectra of H-$ZnGa_2O_4$ at -1.03V and -1.2 V. a) Zn 2p, b) Ga 3d.

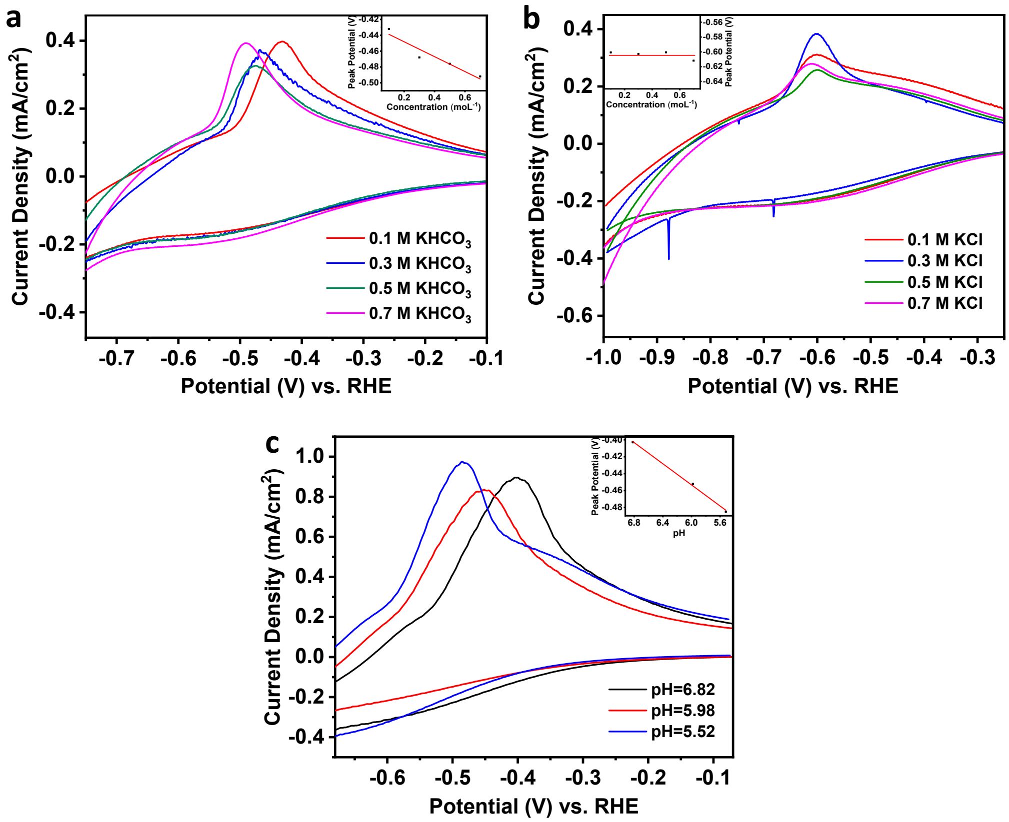

Figure S12. Cyclic voltammogram of the L-$ZnGa_2O_4$ in a) CO_2-saturated $KHCO_3$ solution. b) CO_2-saturated KCl solution. c) 0.1 M CO_2-saturated $KHCO_3$ solution with different pH value. The inset shows the linear relationship between the peak potential and the concentration of a) $KHCO_3$ solution, b) KCl solution, c) protons in 0.1 M $KHCO_3$ solution.

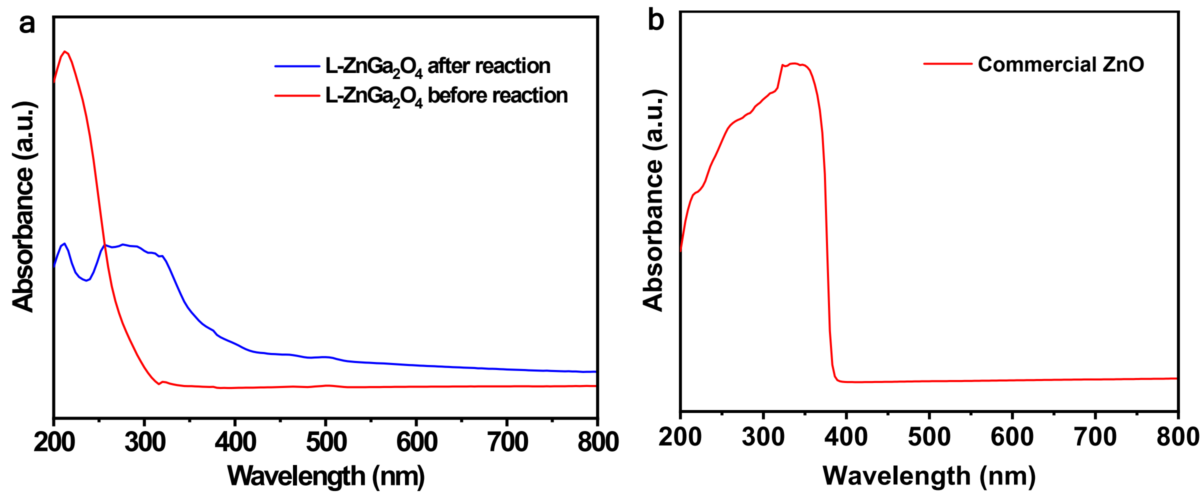

Figure S13. Ultraviolet-visible (UV-vis) absorption spectrum of a) L-$ZnGa_2O_4$ after and before reaction, b) commercial ZnO.

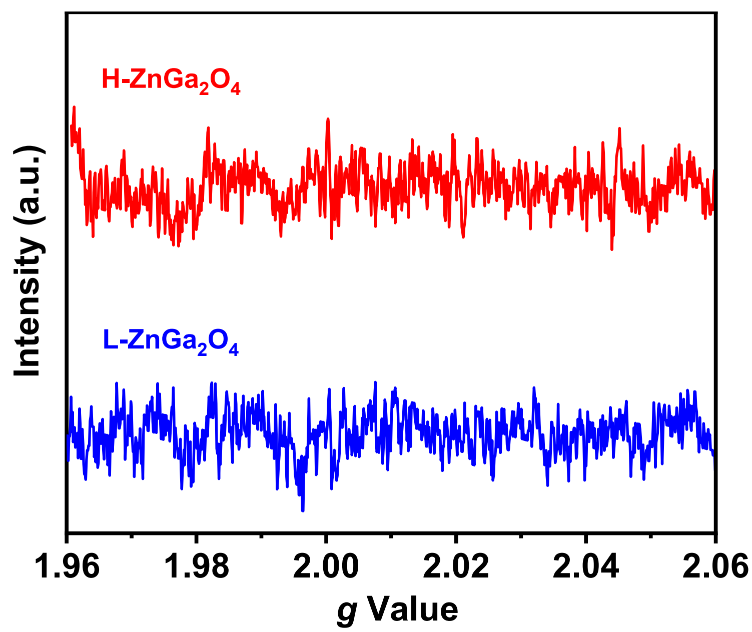

Figure S14. EPR for L-$ZnGa_2O_4$ and H-$ZnGa_2O_4$.

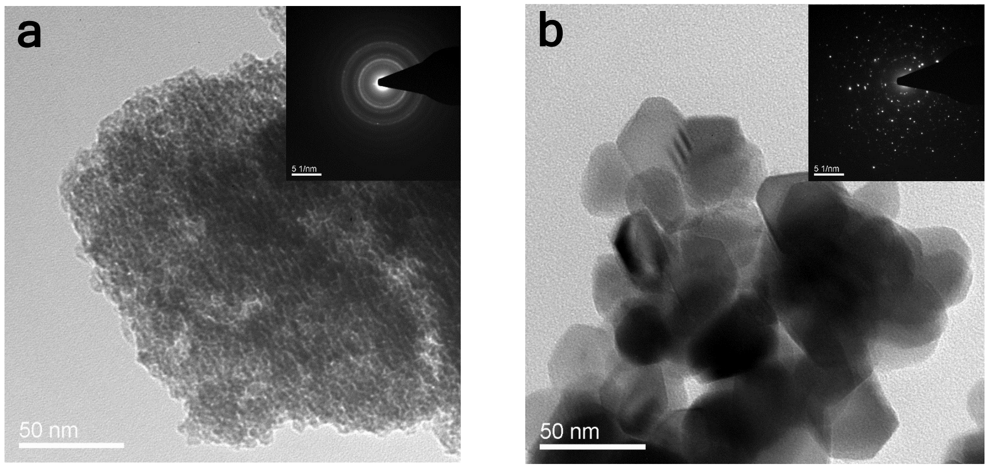

Figure S15. a) High-magnification TEM image of L-$ZnGa_2O_4$ after reaction. (insert: SAED pattern of porous $ZnGa_2O_4$) and b) H-$ZnGa_2O_4$ after reaction. (insert: SAED pattern of nonporous $ZnGa_2O_4$).

Table S1. Comparison of CO_2 electrochemical reduction performances on different Zn catalysts.

	Electrolyte	**Main Product**	**Potential (V) vs. RHE**	**Faradaic Efficiency (%)**	**Reference**
Zn^{2+}/ $Zn^{\delta+}$	0.1 M $KHCO_3$	CO	-0.8	96	This work
Zn Dendrites	0.5 M $NaHCO_3$	CO	-1.1	79	[1]
Zn nanoplates	0.5 M $NaHCO_3$	CO	-0.93	57	[2]
Zn nanoplates	0.5 M NaCl	CO	-1.09	93	[2]
Hexagonal Zn	0.5 M $KHCO_3$	CO	-0.95	85.4	[3]
Hexagonal Zn	0.5 M KCl	CO	-1.05	95.4	[3]
Reduced ZnO	0.25 M K_2SO_4	CO	-1.2	92	[4]
Zn nanosheets	0.5 M $NaHCO_3$	CO	-1.13	86	[5]
Zn nanoparticle	0.5 M $NaHCO_3$	$HCOO^-$	-1.93	87.1	[6]

[1] J. Rosen, G. S. Hutchings, Q. Lu, R. V. Forest, A. Moore and F. Jiao, *ACS Catal.,* 2015, **5**, 4586.
[2] F. J. Quan, D. Zhong, H. C. Song, F. L. Jia and L. Z. Zhang, *J. Mater. Chem. A*, 2015, **3**, 16409.
[3] D. H. Won, H. Shin, J. Koh, J. Chung, H.S. Lee, H. Kim and S. I. Woo, *Angew. Chem. Int. Ed.*, 2016, **55**, 9297.
[4] X. L. Jiang, F. Cai, D. F. Gao, J. H. Dong, S. Miao, G. X. Wang and X. H. Bao, *Electrochemistry Communications*, 2016, **68**, 67.

[5] T. T. Zhang, X. F. Li, Y. L. Qiu, P. P. Su, W. B. Xu, H. X. Zhong and H. M. Zhang, *Journal of Catalysis*, 2018, **357**, 154.
[6] T. T. Zhang, H. X. Zhong, Y. L. Qiu, X. F. Li and H. M. Zhang, *J. Mater. Chem. A*, 2016, **4**, 16670.

Table S2. The pH of CO_2-saturated $KHCO_3$, KCl electrolyte with different concentrations.

Electrolyte	Concentration (M)	pH
CO_2-saturated $KHCO_3$	0.1	6.82
CO_2-saturated $KHCO_3$	0.3	7.23
CO_2-saturated $KHCO_3$	0.5	7.45
CO_2-saturated $KHCO_3$	0.7	7.62
CO_2-saturated KCl	0.1	3.98
CO_2-saturated KCl	0.3	4.03
CO_2-saturated KCl	0.5	4.05
CO_2-saturated KCl	0.7	3.91